Interplay between pairing and tensor effects in the $N = 82$ even-even isotone chain.

M. Anguiano, R. N. Bernard, A. M. Lallena

Departamento de Física Atómica, Molecular y Nuclear,

Universidad de Granada, E-18071 Granada, Spain

G. Co'

Dipartimento di Matematica e Fisica "E. De Giorgi",

Università del Salento and, INFN Sezione di Lecce,

Via Arnesano, I-73100 Lecce, Italy

V. De Donno

Dipartimento di Matematica e Fisica "E. De Giorgi",

Università del Salento, Via Arnesano, I-73100 Lecce, Italy

(Dated: July 26, 2016)

Abstract

We investigate the ground state properties of the nuclei belonging to the isotonic chain $N = 82$. The pairing effects have been taken into account by considering a Hartree–Fock–Bogoliubov and also a Hartree–Fock plus Bardeen–Cooper–Schrieffer approaches. We consider finite-range interactions to obtain stability of the results against the changes of the dimensions of the single particle configuration space. Our results reproduce very well the available experimental data of binding energies and charge radii. The study of the particle number fluctuation indicates a remarkable sensitivity of the pairing effects to the presence of tensor terms in the interaction. In some situations, they reduce the pairing effects, and produce shell closure phenomena. The experimental behavior of the energy difference between neutron single particle states up to $A = 140$ is described only if the tensor force is considered.

PACS numbers:

I. INTRODUCTION

In the solar system, the abundance distribution of nuclei generated by r-process shows a peak around $A = 130$ [1]. The common interpretation of this observation is related to the shell closure when the neutron number, N, is 82 [2]. On the other hand, recent experimental data of nuclei far from stability indicate important changes in the shell structure [3], and motivate more detailed studies of nuclei with neutron excess in the region of Sn isotopes and $N = 82$ isotones. It is nowadays an experimental evidence that the sequence of single particle (s.p.) states changes with the ratio N/Z [4]. This implies that new magic numbers emerge and other ones disappear [5–7].

Starting from the seminal works of Otsuka *et al.* [8, 9] it has been established a relation between the trend in the evolution of the nuclear shells and the tensor part of the nucleon-nucleon interaction. The inclusion of the tensor force improves the description of the new and old magic numbers [10].

In this article we carry out a theoretical study of the isotone chain of even-even nuclei with $N = 82$ around the ^{132}Sn doubly magic nucleus. We adopt a description based on the spherical symmetry of these nuclei, and we consider the pairing in the proton sector only, since the neutron number is magic.

The simplest mean-field approach that takes into account the pairing effects is the Bardeen–Cooper–Schrieffer (BCS) model [11–13]. Inputs of this model are a set of s.p. states and a pairing nucleon-nucleon interaction. The solution of the BCS pairing equations produces partial occupation probabilities of each s.p. state which are used to calculate various ground state observables.

A more involved, and consistent, treatment of the pairing is provided by the Hartree–Fock–Bogoliubov (HFB) theory [14]. In this case, the only input required is the effective nucleon-nucleon interaction. The s.p. states and their occupation probabilities are obtained in a unique step by solving a system of integro-differential non-linear equations [12].

Recently, we have developed a Hartree–Fock plus BCS (HF+BCS) model [15] which uses the same effective, finite-range, nucleon-nucleon interaction in the two steps of the calculation, HF and BCS. For this reason, the only input of our approach is the effective nucleon-nucleon interaction whose parameters have been fixed once forever in a global fit. Specifically, we used nucleon-nucleon interactions of Gogny type [14, 16, 17]. We compared

our results with those obtained in HFB calculations by using the same interaction [18, 19]. The agreement between the two types of calculation is very good [15, 20].

It is worth noticing that the finite range of the interaction ensures the stability of the BCS results against the enlargement of the s.p. configuration space. This occurs, of course, after that certain dimensions of the s.p. configuration space have been reached. On the contrary, the use of zero-range forces always requires renormalisation procedures, eventually by using different interactions in the HF and in the BCS calculations [21].

The aim of the present article is to study the evolution of the ground state properties of the isotone chain with $N = 82$ by considering the presence of the tensor interaction together with that of the pairing force. We carry out our investigation by considering the finite-range interactions introduced in Ref. [22] where tensor terms have been added to well defined parameterizations of the Gogny interactions. We investigate the emergence and disappearance of magic numbers when the tensor interaction is included at the HF level. To be sure that our results are due to the presence of the tensor term, and not to its specific implementation in an effective theory, we calculated the various quantities presented in the work with both HFB and HF+BCS approaches. To the best of our knowledge, in addition to our work, only the calculations of Ref. [23] have considered, up to now, the tensor terms of finite-range effective forces in HFB calculations.

In Sec. II we present the basic ideas of our nuclear structure model, and we describe how we calculate the quantities, and the observables considered in our work. We discuss our results in Sec. III. We first show binding energies and proton and neutron root mean square (rms) radii for the full chain of isotones. Then, we present the fluctuation of the particle number obtained with and without tensor interaction to study the shell closure. Finally, we compare our results with the, recently measured, empirical data [24, 25], which show the behavior of the energy difference between the neutron $1i_{13/2}$ and $1h_{9/2}$ s.p. states as a function of the proton number. In Sec. IV we summarize our results and we draw our conclusions.

II. THE MODELS

We recall here below some basic points of our HF+BCS approach which is described with more details in Ref. [15]. We first generate a set of s.p. wave functions in a spherical basis

by solving the HF equations. When the iterative method described in Ref. [26] has reached convergence, the direct, Hartree, and exchange, Fock-Dirac, potentials are built by using the s.p. wave functions below the Fermi surface and inserted in the integro-differential HF equations to generate the set of s.p. wave functions above it.

Each s.p. state $|k\rangle \equiv |\epsilon_k; n_k l_k j_k m_k\rangle$ is characterized by the principal quantum number n_k, the orbital angular momentum l_k, the total angular momentum j_k, its z axis projection m_k and the energy ϵ_k. These s.p. states are used as the starting point to solve the BCS equations. From their solution, we obtain the occupation probabilities v_k^2 of each s.p. state. The knowledge of v_k and u_k, normalized such that $v_k^2 + u_k^2 = 1$, and of the s.p. wave function $\phi_k(\mathbf{r})$, allows us to evaluate the expectation values of various quantities with respect to the BCS ground state.

For example, we calculate the particle number fluctuation defined as

$$\langle (\Delta N)^2 \rangle \; = \; \langle \mathrm{BCS} | \hat{N}^2 | \mathrm{BCS} \rangle \; - \; \langle \mathrm{BCS} | \hat{N} | \mathrm{BCS} \rangle^2 \; = \; 4 \sum_k (2j_k + 1) \, u_k^2 \, v_k^2 \, , \tag{1}$$

to study the pairing effect. In the previous equation, $\hat{N}$ represents the particle number operator. In the following, we shall indicate as $\langle (\Delta N)^2 \rangle_{\mathrm{t}}$ the result obtained when the sum of Eq. (1) is restricted to proton, t=p, or neutron, t=n, s.p. states, and we shall compare the values obtained in our HF+BCS approach with those of the HFB calculation.

In the next section we shall present results related to the global energy of the HF+BCS ground state obtained as

$$E \; = \; \frac{1}{2} \sum_k (2j_k + 1) \; \left[v_k^2 (\epsilon_k + \langle k | T | k \rangle) \; - \; u_k \, v_k \, \Delta_k \right] \, , \tag{2}$$

where we have indicated with T the kinetic energy operator. In the above equation, the symbol Δ_k is defined as

$$\Delta_k \; = \; - \frac{1}{\sqrt{2j_k + 1}} \; \sum_i \sqrt{2j_i + 1} \, u_i \, v_i \, \langle ii0 | V | kk0 \rangle \, , \tag{3}$$

where $|kk'0\rangle$ indicates a state where the $|k\rangle$ and $|k'\rangle$ s.p. states are coupled to total angular momentum $J = 0$, and V is the pairing interaction.

In our HF+BCS model, the matter density distribution is obtained as

$$\rho(r) \; = \; \sum_k v_k^2 \, |\phi_k(\mathbf{r})|^2 \; = \; \frac{1}{4\pi} \sum_k (2j_k + 1) \, v_k^2 \, |R_k(r)|^2 \, , \tag{4}$$

where we have indicated with R_k the radial part of the s.p. wave function normalized as

$$\int_0^\infty r^2 \, |R_k(r)|^2 \, \mathrm{d}r \, = \, 1 \, . \tag{5}$$

We obtain the proton, ρ_p, and neutron, ρ_n, density distributions by selecting the corresponding s.p. states in the sum of Eq. (4). From the above distributions we determine the rms radii by calculating

$$\langle r^2 \rangle_\mathrm{t}^{1/2} \, = \, \left[\frac{\displaystyle\int_0^\infty r^4 \, \rho_\mathrm{t}(r) \, \mathrm{d}r}{\displaystyle\int_0^\infty r^2 \, \rho_\mathrm{t}(r) \, \mathrm{d}r} \right]^{1/2} \quad , \tag{6}$$

where the subindex t identifies protons, p, or neutrons n radii.

In our model the HF equations are solved by imposing bound boundary conditions at the edge of an r-space box [26–28]. In this manner all the s.p. states forming the working configuration space are bound, even those with positive energy. The size of the s.p. configuration space should be large enough to ensure the stability of the BCS results. From the numerical point of view, the use of finite-range interactions automatically generates the stability of these results without adding additional renormalisation parameters [29]. In our BCS calculations we have considered all the s.p. states with energies up to 10 MeV. We have checked that this guarantees the stability of the BCS energy (2) within the keV range.

The HFB calculations have been performed by using the technique developed by Robledo *et al.* [30, 31], based on the gradient method. The approximated second order gradient method is applied to minimize the energy functional in the constrained HFB method. The time reversal, simplex and axial symmetries are preserved in our HFB calculations. The HFB equations are solved in the three dimensional harmonic oscillator basis of the Fock space, and the oscillator length parameters are equal to 2.1 fm in all directions. This allows the analysis of spherical nuclei. In our HFB calculations the Coulomb term is exactly treated, i.e. we do not use the commonly adopted Slater approximation [19]. The HFB results we shall present in the following have been obtained by using a configuration space composed by 10 major harmonic oscillator shells.

Our calculations have been carried out by using effective finite-range interactions of Gogny type [14, 16], which can be expressed as a sum of central, V_C, spin-orbit, V_SO, density dependent, V_DD, and Coulomb, V_Coul, terms

$$V(1,2) \, = \, V_\mathrm{C}(1,2) \, + \, V_\mathrm{SO}(1,2) \, + \, V_\mathrm{DD}(1,2) \, + \, V_\mathrm{Coul}(1,2) \, . \tag{7}$$

The central term, which depends on the spin and the isospin of the two interacting nucleons, has a finite range, while the spin-orbit and density dependent terms are of zero-range type.

In this article we shall present results obtained with the traditional D1S interaction, and its extension D1ST2a which includes tensor terms [22]. We have carried out calculations by using the more recent D1M parameterization of the force [17]. The results obtained with this force are very similar to those obtained with the D1S interaction, and for this reason, we do not show them in this paper.

The tensor terms contained in the D1ST2a interaction [22] can be expressed in the form

$$V_{\rm T}(1,2) = [\mathcal{V}_{\rm T1} + \mathcal{V}_{\rm T2}\, \boldsymbol{\tau}(1)\cdot\boldsymbol{\tau}(2)]\; S_{12}\; \exp[-(\mathbf{r}_1-\mathbf{r}_2)^2/\mu_{\rm T}]\;, \tag{8}$$

where we have indicated with S_{12} the usual tensor operator, and with $\mathcal{V}_{\rm T1}$, $\mathcal{V}_{\rm T2}$ and $\mu_{\rm T}$ real numbers whose values are free parameters. The parameters of the tensor interaction have been chosen to reproduce the energy of the first 0^- state of the nucleus ^{16}O and the energy difference between the neutron $1f_{7/2}$ and $1f_{5/2}$ s.p. states of ^{48}Ca without changing the values of the other parameters of the D1S force. By using this procedure we chose $\mathcal{V}_{\rm T1} = -77.5$ MeV, $\mathcal{V}_{\rm T2} = 57.5$ MeV and $\mu_{\rm T} = 1.2$ fm. This last value has been chosen to coincide with the longest range of the two gaussians of the D1S Gogny interaction.

In the BCS calculations we have followed the procedure commonly adopted in the pairing sector of the HFB calculations when Gogny type interactions are used [14, 16, 18], and we have considered only $V_{\rm C}$, the central, finite-range term of Eq. (7). This means that in all our calculations, either HFB or HF+BCS, the tensor term is present only at the HF level, and not in the pairing sector. In any case, we point out that this is the first time that the contribution of tensor forces is considered in HFB calculations done with the axial code developed in [30, 32].

III. RESULTS

In order to clarify the quality of our calculations we show in Fig. 1 the binding energies and the proton and neutron radii of the nuclei under study. The circles and the squares indicate, respectively, the HF+BCS and HFB results obtained with the D1S interaction. The triangles, in the panel (a), show the experimental values taken from Ref. [33]. The largest relative difference between the available experimental data and our results is about

2%. In panel (b) of the figure we show the proton and neutron rms radii, (see Eq. (6)). The results of the two types of calculations, HF+BCS (circles) and HFB (squares), essentially overlap for all the nuclei investigated. For these two observables the effects of the tensor are within the numerical accuracy of the calculations, and for this reason, in the figure, we do not show the binding energies and radii obtained with the D1ST2a interaction.

A quantity extremely sensitive to both tensor and pairing forces is the particle number fluctuation $\langle(\Delta N)^2\rangle$, defined in Eq. (1). This quantity goes to zero if the pairing effects are negligible due to the fact that the energy gap between the last occupied and the first empty s.p. level in the extreme mean-field picture is too large. Therefore a zero value of $\langle(\Delta N)^2\rangle$is an indication of shell closure. In the isotone chain under study the number of neutrons is fixed and corresponds to a magic number, 82. In this case $\langle(\Delta N)^2\rangle_{\rm n}$ is zero, therefore we shall consider only the proton number fluctuation, $\langle(\Delta N)^2\rangle_{\rm p}$.

In Fig. 2 we show the $\langle(\Delta N)^2\rangle_{\rm p}$ values of the $N = 82$ isotone chain calculated with the D1S interaction, panel (a), and with the D1ST2a interaction, panel (b). In the figure, the squares show the results found in HFB calculations, and the circles those calculated with HF+BCS.

In each of the two panels, the HFB and HF+BCS results are very similar. The comparison of the results of the two panels indicates that the presence of the tensor produces additional shell closures for the ^{122}Zr, ^{140}Ce and ^{146}Gd nuclei. These effects are due to the full occupation of the proton $2p_{1/2}$, $2d_{5/2}$ and $1g_{7/2}$ s.p. levels.

The tensor effects we have pointed out become evident in the behavior of the nucleon separation energies. We present in the panel (a) of Fig. 3 the two-proton separation energies

$$S_{\rm 2p}(Z,N) \,=\, E(Z-2,N) \,-\, E(Z,N) \ , \tag{9}$$

calculated for the full isotone chain. In this figure we show the results obtained with HFB using the D1S (black squares) and the D1ST2a (white squares) forces. Those found with the HF+BCS approach are indistinguishable on the scale of the figure. The red triangles indicate the available experimental data extracted from the compilation of Refs.[33, 34].

The lines in our figures have been drawn to guide the eyes, and they become extremely useful in this case because they emphasize the changes of slope of the various calculations. For the dashed line, linking the results obtained with the D1S interaction, the slope changes only in coincidence with the ^{132}Sn nucleus, the only case where in Fig. 2 we observe a zero

value of $\langle(\Delta N)^2\rangle_{\rm p}$. The slope of the solid line, corresponding to the results obtained by including tensor terms, shows three additional changes in coincidence with $A = 122$, 140 and 146, where, in Fig. 2, we have observed that $\langle(\Delta N)^2\rangle_{\rm p}$ is zero. To have a better view of these behaviors we show in the panel (b) of Fig. 3 the quantity

$$\Delta S_{2\rm p}(Z,N) \,=\, \frac{1}{2}\left[S_{2\rm p}(Z-2,N) \,-\, S_{2\rm p}(Z,N)\right] \,, \tag{10}$$

which emphasises the change of slope by presenting a peak in coincidence with the isotone following that where the slope changes. Both types of calculation show a peak at $A = 134$, therefore, the change of slope appears at $A = 132$ which is the closed shell isotone. The full line of panel (b), linking the results obtained by using the tensor force, shows additional, even if smaller, peaks corresponding to $A = 124$, 142 and 148, indicating the change of slope, and the eventual shell closure, for $A = 122$, 140 and 146 isotones. The comparison with the available experimental data shows a better agreement with the D1S results rather than with those obtained with D1ST2a.

Since in our calculations the tensor force has been used only in the evaluation of the HF s.p. basis, the effects we have observed are only due to the modifications of the energy of the proton s.p. levels which, consequently, affect the pairing contributions. To have a better insight of this combination of effects, we present in Fig. 4 the occupation numbers v^2, panel (a), and the energies ϵ, panel (b), of the proton $1g_{7/2}$ and $2d_{5/2}$ s.p. states as a function of the mass number A, as we have obtained in HF+BCS calculations.

The white and black circles show the results obtained with the D1S and the D1ST2a interactions, respectively. For both states the smooth behavior of v^2 is strongly modified by the tensor force which produces a sharp increase. The main effect of the tensor interaction is due to its action between the neutron $1h_{11/2}$ s.p. level and the two proton levels considered in the figure. The energy of the proton $1g_{7/2}$ level decreases, while that of the $2d_{5/2}$ level remains essentially unchanged. As a consequence of these changes, the energy difference between these two proton levels increases when the tensor is included, and this reduces the size of the pairing effects.

The D1ST2a interaction has been constructed on the D1S force by adding the tensor interaction given in Eq. (8) composed by a pure tensor term, related to the $\mathcal{V}_{\rm T1}$ parameter, and a tensor-isospin term, related to the $\mathcal{V}_{\rm T2}$ parameter. In order to understand the relevance of each of these terms in the effects we have discussed so far, we have investigated their

individual role on the proton number fluctuation, $\langle(\Delta N)^2\rangle_{\rm p}$.

The results of this study with the HF+BCS approach are shown in Fig. 5 where we compare the values of $\langle(\Delta N)^2\rangle$, Eq. (1), obtained by using the full D1S and D1ST2a interactions, represented by the white and black circles respectively, with those found using the pure tensor (blue triangles) and tensor-isospin (red squares) terms. These latter results have been obtained by setting $\mathcal{V}_{\rm T2} = 0$ and $\mathcal{V}_{\rm T1} = 0$ in Eq. (8), respectively.

There is a remarkable similarity between the D1S results and those obtained only with the pure tensor term. On the other hand, the values obtained with the full D1ST2a force are rather similar to those obtained by using only the tensor-isospin term. We remark, however, that in the last case the shell closure of ^{132}Sn and ^{146}Gd does not appear. In our parameterization of the tensor force these effects are produced, at least in some cases, by the interference between the two terms of Eq. (8).

Since the main effect of the tensor force is on the s.p. energies, we tested the predictions of our model against the empirical data related to the differences between the energies of the neutron $1i_{13/2}$ and $1h_{9/2}$ s.p. states, and between the neutron $2f_{5/2}$ and $2f_{7/2}$ s.p. states. The results of our HF+BCS calculations are shown in the Fig. 6, where the white and black circles have been obtained by using the D1S and D1ST2a interactions, respectively.

In the panel (a), where we show the energy differences between the neutron $1i_{13/2}$ and $1h_{9/2}$ s.p. states, we show two types of empirical data, presented by the blue triangles and red squares. The former have been calculated as difference between the energies of the lowest $13/2^+$ and $9/2^-$ excited states of the corresponding $N = 83$ nuclei, taken from the compilation of Ref. [34]. The red squares are the centroid energies of the s.p. strengths extracted in (d, p) pick-up reactions, and given in Ref. [24].

The general trend of the experimental data is reproduced, at least up to $A = 140$, only by the calculations carried out with the tensor force, in agreement with the results of Otsuka et al. [8, 24, 25]. This behavior can be understood by considering the occupation probabilities v^2 shown in Fig. 4. The observable we are studying is related to the filling of the proton $1g_{7/2}$ s.p. state. When the number of protons increases, and therefore the occupation of this level, the tensor interaction between this s.p. level and the neutrons levels is enhanced. Since the $1g_{7/2}$ state has $j = l - 1/2$, the tensor force lowers the energy of the neutron $1i_{13/2}$ level, and acts with opposite sign on the energy of the $1h_{9/2}$ level. Consequently, the energy difference between these two levels becomes smaller, as indicated by the black circles in the

figure. For $A = 140$ the proton $1g_{7/2}$ state is completely full, therefore the protons start to fill the $2d_{5/2}$ s.p. state, which has opposite effect on the neutron levels since $j = l + 1/2$. This explains the change of slope observed in our results, which, on the other hand, is absent in the empirical data.

In the panel (b) of Fig. 6 we compare our HF+BCS results with the empirical data related to the energy difference between the neutron $2f_{5/2}$ and $2f_{7/2}$ s.p. states. The meaning of the symbols and of the lines is the same as in the upper panel. The behavior of the D1ST2a results is completely different with respect to that shown by the results obtained with the D1S interaction. The tensor interaction between the protons lying on the $1g_{7/2}$ state increases the energy of the neutron $2f_{5/2}$ level and lowers that of the neutron $2f_{7/2}$ state. The figure shows an increase of the difference between the energy of these two states, a behavior similar to that of the empirical data. In analogy to what happens in upper panel, our HF+BCS calculations change behavior at $A = 140$, when the proton $1g_{7/2}$ s.p. level is completely full. After $A = 140$ we observe a change of slope related to the filling of the proton $2d_{5/2}$, and now the tensor force has opposite sign effects on the two neutron levels considered.

IV. SUMMARY AND CONCLUSIONS

We have studied the ground state properties of the $N = 82$ isotonic chain which is particularly interesting for astrophysical r-processes. Our study has been conducted within a mean-field framework where the pairing interaction has been taken into account by using HFB and HF+BCS approaches. Our aim was to investigate the role of the tensor force in the shell structure of the isotone chain, and, to be sure of handling with real tensor force effects and not with effects related to the specific implementation of the force, we have carried out the calculations with both approaches. We should point out that our HFB calculations, together with those of [23], are the only ones where a finite range tensor interaction is considered, and certainly they are the first ones which used the technology of Ref. [32] for this purpose.

Our calculations have been carried out by using finite-range Gogny interactions, in both the Hartree-Fock and the pairing sectors. This ensures the stability of the results against the increase of the s.p. configuration space. We used the D1S interaction and the D1ST2a force which add to the D1S interaction a pure tensor and a tensor-isospin term, as indicated in Eq.

(8). Since the parameters of these forces have been selected in the literature, we do not have any free parameter to play with, and, in this sense, we may state that our calculations are parameter free. The quality of our calculations has been clarified by showing the excellent agreement between our results and experimental binding energy of the $N = 82$ isotone chain.

The effects of the tensor force have been emphasized in the study of the particle fluctuation $\langle(\Delta N)^2\rangle$, defined in Eq. (1). The comparison between calculations done with and without tensor force indicates that the presence of the tensor produces new shell closure for A=122, 140, 146. We should point out that, at least for the ^{146}Gd nucleus, there have been empirical claims about its shell closure [35], which have triggered a set of study of this nucleus, see [36] and references therein.

We have analyzed in detail the mechanism associated to the presence of the tensor force which produces the emergence of these new shell closure. The tensor force increases the proton energy gap, and this reduces the effects of the pairing generating the new shell closure. The main responsible of this effect is the tensor-isospin part of our tensor force (8). However, the presence of the pure tensor term is not negligible since it generates strong interference effects together with tensor-isospin term.

We searched for a phenomenological validation of these results by calculating the evolution in the isotone chain of the difference between the energy of two neutron s.p. states which is also empirically known. While the results without tensor fail completely in describing the data, those obtained with the tensor force have the correct behavior up to a certain value of the mass number, $A = 140$ in the specific cases studied. However, the general agreement is not satisfactory, from both the quantitative and qualitative point of view.

We conclude by stating that a detailed description of the shell evolution in the $N = 82$ isotone chain, and more in general, in the experimentally unexplored regions of the isotope chart, requires the inclusion of the tensor term in the effective interaction to be used. The present situation is, however, not satisfactory and it requires additional work. Certainly it will be necessary to include the tensor force also in the pairing sector, even though our first, preliminary, results seem to indicate small effects. Second, and probably more relevant, it is necessary a more systematic and global fit of observables to choose the parameters of the tensor force. Whether this should be done as we have done, maintaining fixed the parameters values of the full force (7) and selecting only the parameters of the tensor force, or involving in a global fit all the parameters of the new force, is matter of discussion, and investigation.

Acknowledgments

R. N. B. acknlowledges the support from CPAN (CSD2007-00042). Financial support from the Junta de Andalucía (FQM0220), the Spanish Ministerio de Economía y Competitividad (FPA2012-31993), and the European Regional Development Fund (ERDF) is gratefully acknowledged.

[1] I. U. Roederer, et al, Ast. Jour. Lett. 747 (2012) L8.

[2] B. Pfeiffer, K.-L. Kratz, F.-K. Thielemann, W. Walters, Nucl. Phys. A 693 (2001) 282.

[3] C. R. Hoffman, et al., Phys. Lett. B 672 (2009) 17.

[4] J. P. Schiffer, et. al., Phys. Rev. Lett. 92 (2004) 162501.

[5] A. Obertelli, S. Péru, J.-P. Delaroche, A. Gillibert, M. Girod, H. Goutte, Phys. Rev. C 71 (2005) 024304.

[6] K. J. Jones, et. al., Nature 465 (2010) 454.

[7] D. Steppenbeck, et al., Nature 502 (2013) 207.

[8] T. Otsuka, T. Suzuki, R. Fujimoto, H. Grawe, Y. Akaishi, Phys. Rev. Lett. 95 (2005) 232502.

[9] T. Otsuka, T. Matsuo, D. Abe, Phys. Rev. Lett. 97 (2006) 162501.

[10] H. Sagawa, G. Colò, arxiv:1401.6691 [nucl-th].

[11] A. Bohr, B. Mottelson, D. Pines, Phys. Rev. 110 (1958) 936.

[12] P. Ring, P. Schuck, The nuclear many-body problem, Springer, Berlin, 1980.

[13] J. Suhonen, From nucleons to nucleus, Springer, Berlin, 2007.

[14] J. Dechargé, D. Gogny, Phys. Rev. C 21 (1980) 1568.

[15] M. Anguiano, A. M. Lallena, G. Co', V. De Donno, J. Phys. G 41 (2014) 025102.

[16] J. F. Berger, M. Girod, D. Gogny, Comp. Phys. Commun. 63 (1991) 365.

[17] S. Goriely, S. Hilaire, M. Girod, S. Péru, Phys. Rev. Lett. 102 (2009) 242501.

[18] J. L. Egido, J. Lessing, V. Martin, L. M. Robledo, Nucl. Phys. A 594 (1995) 70.

[19] M. Anguiano, J. L. Egido, L. M. Robledo, Nucl. Phys. A 683 (2001) 227.

[20] M. Anguiano, A. M. Lallena, G. Co', V. De Donno, J. Phys. G. In press.

[21] M. Bender, P. H. Heenen, P. G. Reinhard, Rev. Mod. Phys. 75 (2003) 121.

[22] M. Anguiano, M. Grasso, G. Co', V. De Donno, A. M. Lallena, Phys. Rev. C 86 (2012) 054302.

[23] H. Nakada, Phys. Rev. C 81 (2010) 027301.

[24] B. P. Kay, S. Freeman, J. P. Shiffer, J. A. Clark, C. Deibel, A. Heinz, Phys. Lett. B 658 (2008) 216.

[25] B. P. Kay, J. P. Schiffer, S. Freeman, C. Hoffman, B. Back, S. Baker, S. Bedoor, T. Bloxham, J. A. Clark, C. M. Deibel, A. Howard, J. C. Lighthall, S. T. Marley, K. E. Rehm, D. K. Sharp,

D. V. Shetty, J. S. Thomas, A. H. Wuosmaa, Phys. Rev. C 84 (2011) 024325.

[26] G. Co', A. M. Lallena, Nuovo Cimento A 111 (1998) 527.

[27] A. R. Bautista, G. Co', A. M. Lallena, Nuovo Cimento A 112 (1999) 1117.

[28] M. Anguiano, G. Co', V. De Donno, A. M. Lallena, Phys. Rev. C 83 (2011) 064306.

[29] S. V. Tolokonnikov, S. Kamerdzhiev, D. Voitenkov, S. Krewald, E. E. Saperstein, Phys. Rev. C 84 (2011) 064324.

[30] L. M. Robledo, G. F. Bertsch, Phys. Rev. C 84 (2011) 014312.

[31] L. M. Robledo, R. Bernard, G. Bertsch, Phys. Rev. C 86 (2012) 064313.

[32] L. M. Robledo, HFBAXIAL code (2002).

[33] G. Audi, A. H. Wapstra, C. Thibault, Nucl. Phys. A 729 (2003) 337.

[34] R. B. Firestone, `http://isotopes.lbl.gov/toi.html`.

[35] Y. Nagai, J. Styczen, M. Piiparinen, P. Kleinheinz, D. Bazzacco, P. V. Brentano, K. O. Zell, J. Blomqvist, Phys. Rev. Lett. 47 (1981) 1259.

[36] L. Caballero Ontanaya, Double octupole states in ^{146}Gd, Ph.D. thesis, Universidad de Valencia - CSIC (Spain), arXiv:1001.3279 (2005).

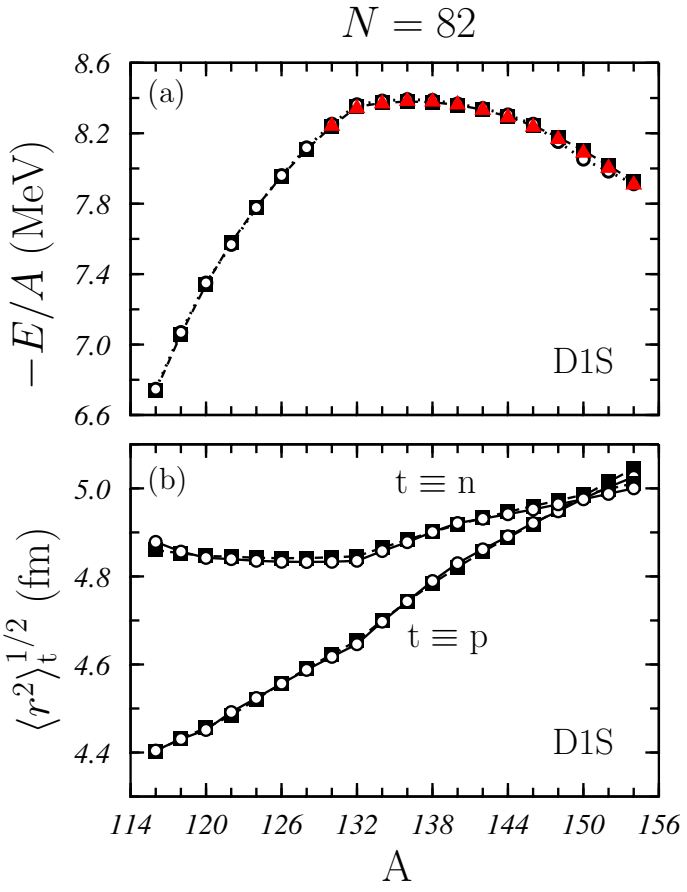

Figure 1: (Color on line) Binding energies per nucleon, upper panel, and rms radii, lower panel, obtained for the even-even isotones with $N = 82$. The white circles show the HF+BCS results and the black squares those obtained with the HFB calculations. The red triangles indicate the experimental binding energies taken from the compilation of Ref. [33]. The lines are drawn to guide the eyes.

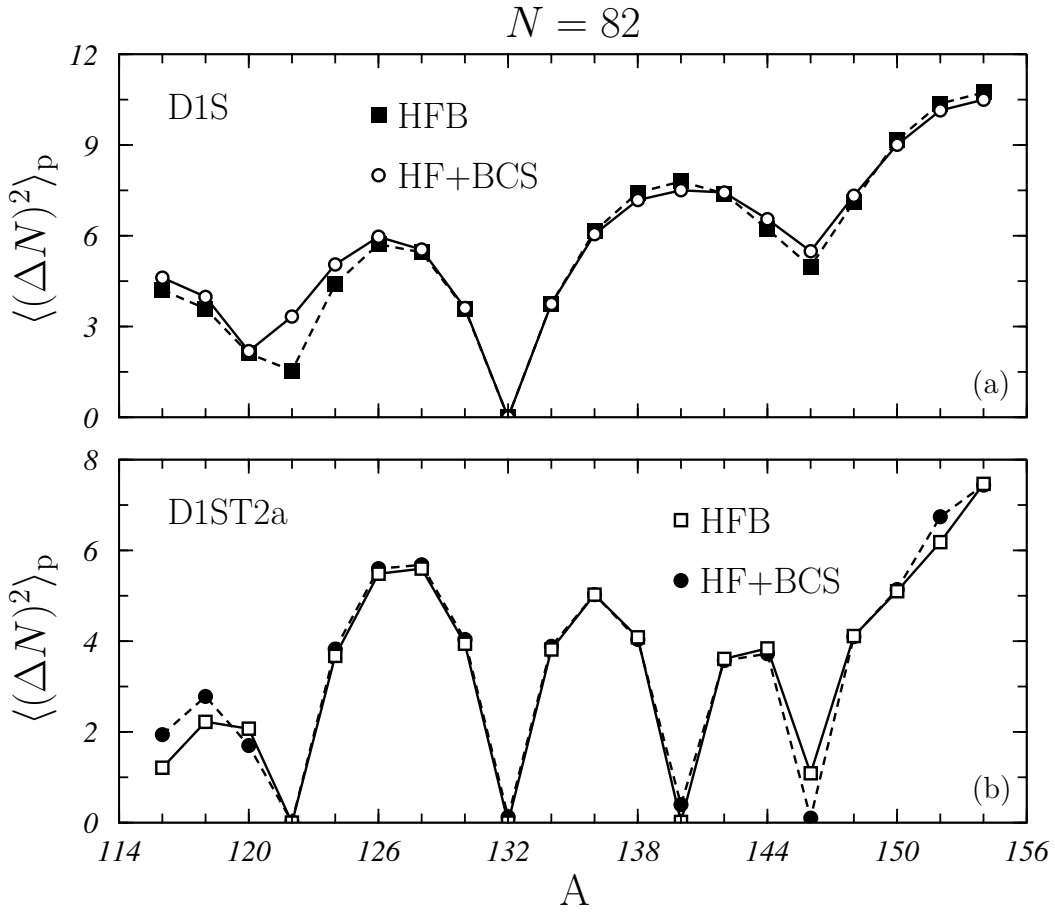

Figure 2: Proton number fluctuation $\langle(\Delta N)^2\rangle_{\rm p}$, Eq. (1), for the various isotones of the $N = 82$ chain. The HF+BCS results are compared to those obtained within HFB model (squares). The upper and lower panels show the values corresponding to the D1S and D1ST2a interactions, respectively. The lines are drawn to guide the eyes.

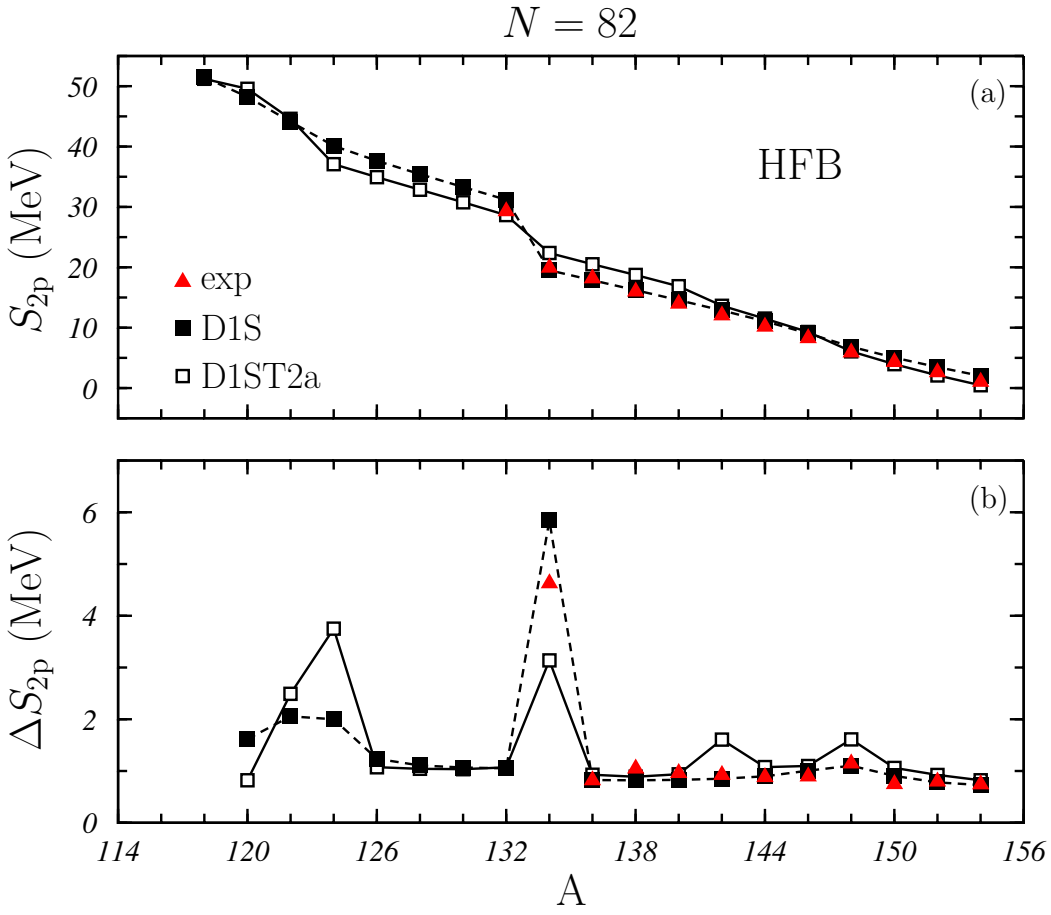

Figure 3: (Color on line) In the upper panel we show the two-proton separation energies S_{2p}, as defined in Eq. (9), and in the lower panel the quantity ΔS_{2p}, as given by Eq. (10), with the D1S and D1ST2a interactions. All the calculations have been carried out within the HFB model. The red triangles are the experimental values [34].

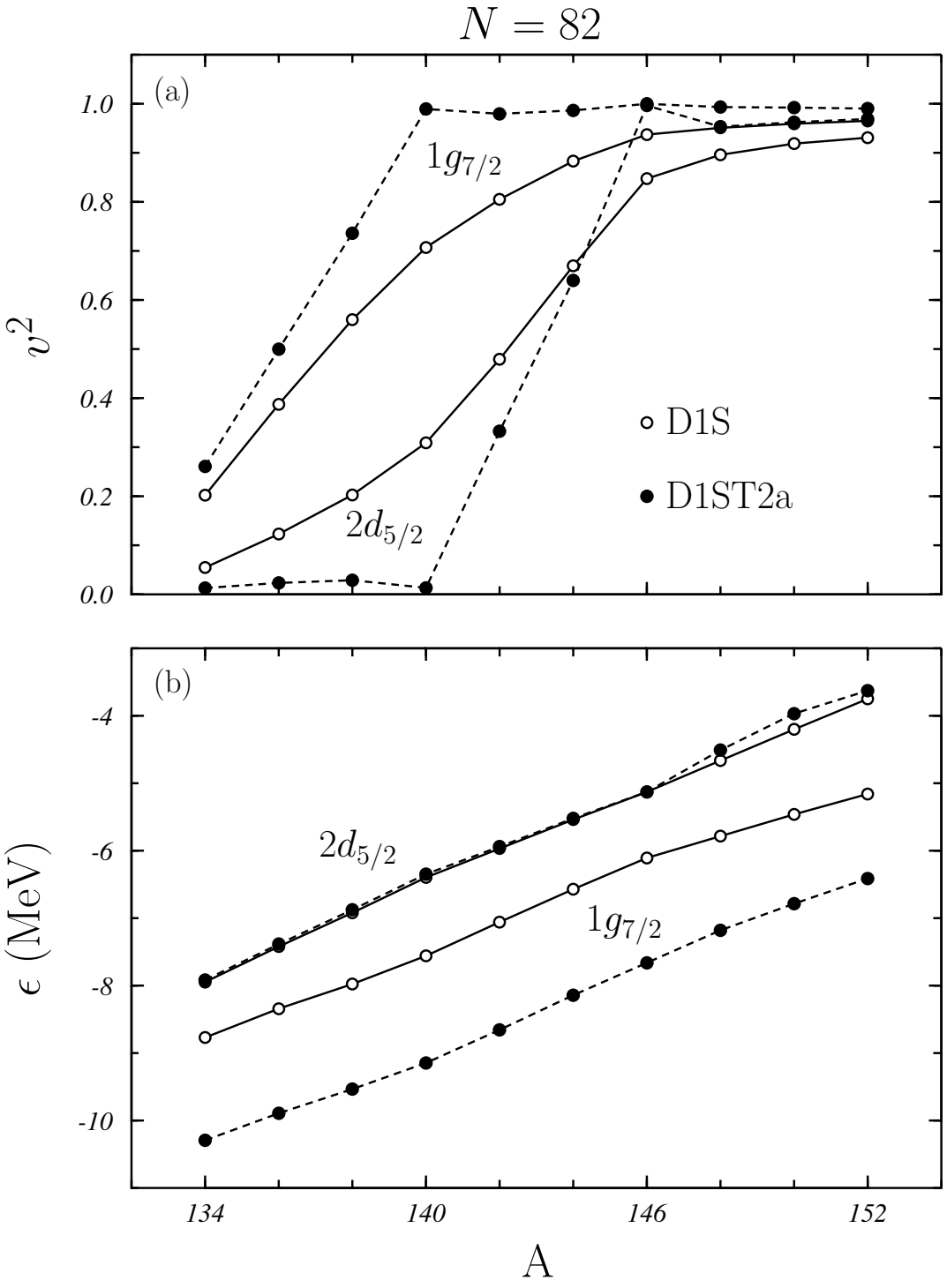

Figure 4: Occupation numbers v^2, panel (a), and s.p. energies ϵ, panel (b), of some proton s.p. states as a function of the mass number. The white circles have been obtained with the D1S interaction and the black ones with the D1ST2a force.

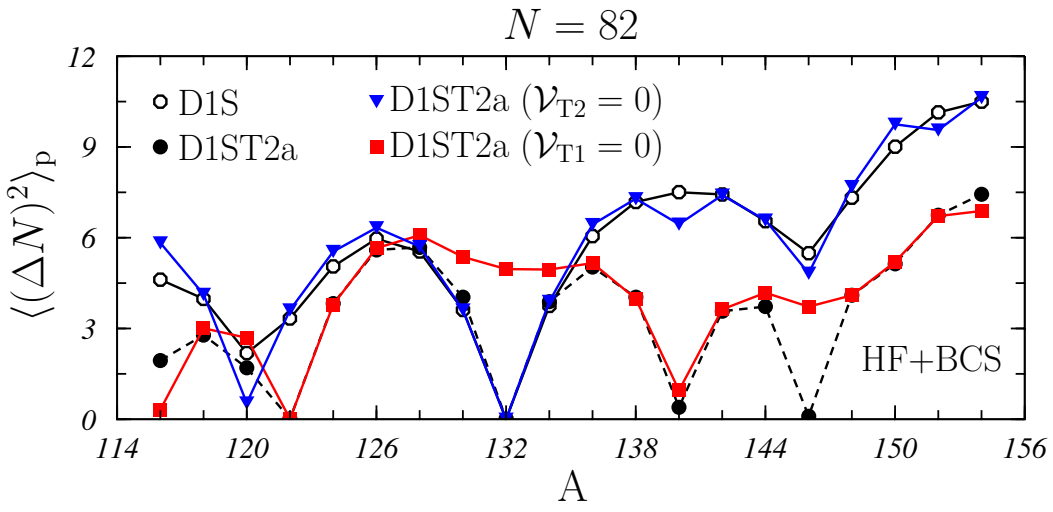

Figure 5: (Color on line) Values of the proton number fluctuation, $\langle(\Delta N)^2\rangle_p$, Eq. (1), for the various isotones of the $N = 82$ chain obtained in HF+BCS calculations. White and black circles are the same as those of Fig. 2 and show the results obtained with the D1S and D1ST2a interactions, respectively. The blue triangles have been obtained by using only the pure tensor term in D1ST2a, i.e. by setting $\mathcal{V}_{T2}$=0 in Eq. (8), while the red squares have been calculated by considering only the tensor-isospin term, i.e. with $\mathcal{V}_{T1}$=0.

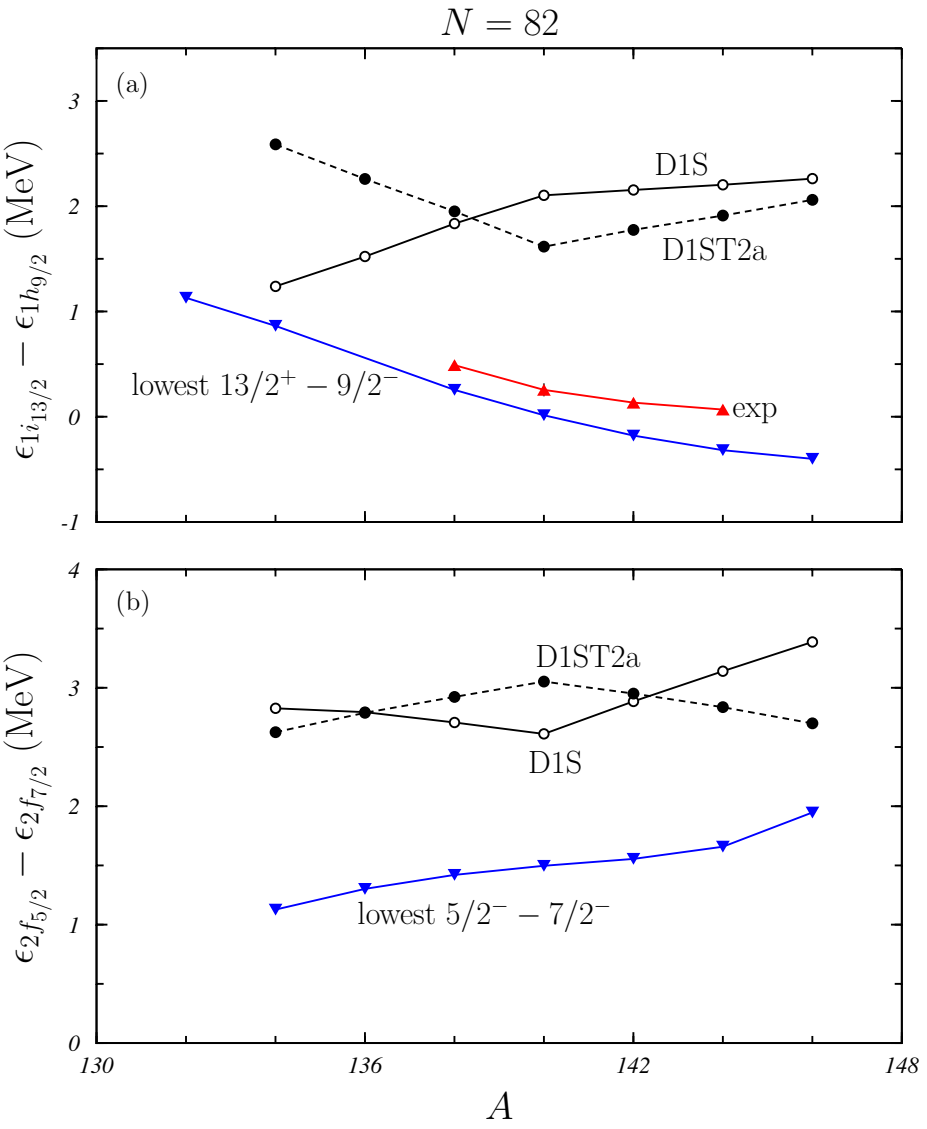

Figure 6: (Color on line) Differences between s.p. energies of the neutron states $1i_{13/2}$ and $1h_{9/2}$, panel (a) and $2f_{7/2}$ and $2f_{5/2}$, panel (b). White and black circles have been obtained by using the D1S and D1ST2a interactions, respectively. The blue triangles indicate the differences between the experimental energies of the corresponding excited states as given in Ref. [34]. The red squares are the centroid energies of the s.p. strengths extracted in (d, p) pick-up reactions [24].